

# Experimental repair technique for glass defects of glass-glass photovoltaic modules – A techno-economic analysis

Mathijs P.M. Tas<sup>a,b,c</sup>, Wilfried G.J.H.M. van Sark<sup>a,\*</sup>

<sup>a</sup> Utrecht University, Copernicus Institute of Sustainable Development, Princetonlaan 8A, 3584 CB Utrecht, the Netherlands

<sup>b</sup> SolSolutions, Hankweg 69, 2641 WV, Pijnacker, the Netherlands

<sup>c</sup> Boldz, Palmstraat 51, 1015 HP AP, Amsterdam, the Netherlands

## ARTICLE INFO

### Keywords:

Glass-glass PV repair  
PV refurbishment  
Experimental repair technique  
Glass defect repair  
Second life of solar

## ABSTRACT

Solar photovoltaic (PV) energy is a crucial supply technology in the envisioned renewable energy system. With enormous amounts of PV modules being installed, some will be affected by early-life failures and the resulting e-waste from PV modules is raising environmental concerns. A failure of growing importance is the defect in the glass layer(s) of glass-glass PV modules. In this research, an experimental glass repair technique for glass-glass PV modules was tested and examined. The PV modules with glass defects under test did not show internal defects in the PV cells, while the repaired specimens performed properly at each phase in the repair process compared to reference modules, the IEC standards and manufacturer warranty. After a damp-heat test the repaired PV modules showed no signs of water ingress, suggesting that the glass layer was restored as a proper barrier. However, definite conclusions should be made with caution since the non-repaired specimens neither showed visible signs of water ingress. While the practical application of the reparation technique has still some uncertainties, glass reparation is found to be technically feasible and effective. Furthermore, economic and energetic analyses indicate that glass defect reparation is economically interesting and energetically desirable.

## 1. Introduction

The photovoltaics (PV) energy industry is currently evolving from a niche market into one of the world's most important energy supply technologies. The combination of cost decrease and improved efficiency will accelerate solar PV deployment to surpass the installed capacity of natural gas and coal by 2024, becoming the world's number one installed energy source for electricity [1]. Renewable energy sources have little related lifetime GHG emissions compared to the current fossil energy system [2]. However, worldwide PV deployment requires enormous amounts of minerals, including scarce minerals such as silver, zinc and indium [3]. As a result, global PV deployment could place these mineral supply chains under tension, leading to higher prices for PV energy which may delay the transition to a fossil-free energy system [1].

A valuable option to limit the reliance on the mineral supply chain, is the recovery of minerals in decommissioned PV modules [4,5]. Decommissioned PV modules contain the minerals required to produce new PV modules. However, not all valuable materials can be recovered. The most energy-intensive parts, photovoltaic cells, cannot be recovered yet [6]. Therefore, the PV sector is developing new measures to decrease

the material requirement, following the reduce-, repair- and recovery-pathway [7,8]. The reparation of defect PV modules is a valuable option in this pathway. Repair techniques can extend the lifetime of decommissioned PV modules, while these modules generally maintain 70%–95% of their initial power output [9].

A growing share of decommissioned PV modules will be glass-glass PV modules, these modules are different from regular glass-back sheet (GBS) modules and replace the traditional polymer back sheet with a glass layer identical to the top glass layer. Glass-glass PV modules currently account for about 15% market share in the PV industry. Nonetheless, these glass-glass designs are predicted to represent up to 50% of the PV market in 2030 [10]. Glass-glass PV modules have a more durable design and higher mechanical strength [11]. Unfortunately, glass-glass PV modules are, similar to regular PV modules, subject to early life failures. A failure of growing concern are defects in the glass layer(s) of PV modules. The scale of decommissioned PV modules with glass defects will increase with the development of solar PV energy [7]. Especially since glass defects arise more frequently at glass-glass PV modules [12,13].

Glass defects can disrupt the insulation of the encapsulant layer and

\* Corresponding author.

E-mail address: [w.g.j.h.m.vansark@uu.nl](mailto:w.g.j.h.m.vansark@uu.nl) (W.G.J.H.M. van Sark).

<https://doi.org/10.1016/j.solmat.2023.112397>

Received 8 March 2023; Received in revised form 16 May 2023; Accepted 18 May 2023

Available online 26 May 2023

0927-0248/© 2023 The Authors. Published by Elsevier B.V. This is an open access article under the CC BY license (<http://creativecommons.org/licenses/by/4.0/>).

PV cells, which can lead to ingress of water. This affects the reliability of the PV modules and might cause safety and/or performance issues [11]. Another potential failure, caused by the mechanical impact which initiated glass breakage, is the formation and enhancement of microcracks in PV cells. This potential impact may cause performance degradation over time and decreased reliability. However, glass defects do not directly imply that PV modules endure internal damage nor that PV modules cannot continue to operate with minimal microcracks. Thus far, glass defects have been regarded as a failure beyond repair and no noticeable attempt has been made to develop repair methods. Even though defects at glass layers do not necessarily affect the performance of PV modules [14].

Glass laminates repair has a long track record in the automotive industry. The most important glass laminates of vehicles, in terms of safety and visibility, are the windshields. Windshield repair is therefore obligated to meet high standards [15]. The automotive industry has developed a repair technique that claims to repair glass defects at windshields to the original strength without visible modifications. The technical effectiveness has made glass defect repair at windshields a well-established procedure [16]. Glass-glass PV modules and car windshields have several shared characteristics which could imply that the windshield repair technique is applicable for glass-glass PV modules. However, the practical use of PV modules and car windshields are very different. Therefore, several challenges distinctive for glass-glass PV modules must be overcome. Consequently, the present study executed and examined an experimental repair method, based on the experience in the automotive industry, for glass-glass PV modules with glass defects.

To the best of our knowledge, no previous research has been executed and examined the possibilities for glass repair of glass-glass PV modules nor regular GBS modules. Most attention in the End-of-Life (EoL) management of PV modules has been going to recycling technologies and material recovery [17]. Research on glass defects has been scarce and limited to the effect, frequency, and origin of the defect [7]. Ultimately, this research aims to add to the scarce scientific knowledge on PV modules repair options, in particular glass-glass PV modules, and aspires to place defect PV modules in a new perspective: from waste to valuable products.

The research paper is structured as follows: section 2 elaborates on the background and relevant theories, followed by section 3 in which the research materials and methods are described. Section 4 presents the research results followed by section 5 which will discuss and conclude these results.

## 2. Background

### 2.1. Double-glass PV modules

In double-glass or glass-glass PV modules the polymer back sheet layer is replaced by a glass layer identical to the top glass, creating a symmetrical “sandwich” structure. The PV cells are in the center, compressed by an encapsulant film and glass layers [11]. The establishment of a glass back layer has several advantages compared to regular GBS modules with respect to an increased reliability, enhanced performance, and improved mechanical strength. Firstly, a significant advantage of glass-glass PV modules is the option for bifacial PV cells. This type of PV cell converts (indirect) light at the rear side of the module into electricity. However, glass-glass PV modules are not bifacial by definition. The application of bifacial PV cells comes at a certain cost, which may not be economically attractive in every application scenario.

Secondly, an important advantage that does apply to all glass-glass PV modules, is the reduced water vapor transmittance (WVT) ratio. Water vapor ingress typically occurs at the more permeable polymer back layer of regular GBS PV modules, and the WVT ratio quantifies the water-permeability of materials. Encapsulated moisture in the internal parts of PV modules affects the reliability and may cause various issues,

e.g., corrosion, delamination and connection failure [11]. The replacement of the back sheet layer with a glass panel drastically reduces the proneness to water penetration. Ingress of water (vapor) at glass-glass PV modules is negligible and restricted to the edge area only [18].

Thirdly, glass-glass PV modules have an increased mechanical strength due to the use of two identical glass panels [18]. The improved mechanical strength makes glass-glass PV modules reliable when confronted with high wind, hail or snow loads. These weather conditions are more frequently observed in harsher climates, therefore glass-glass PV designs are suitable options for these regions [19]. The reliability of the glass-glass PV modules is improved even more by the so-called “Neutral Fiber” zone, i.e., the middle of a symmetrical structure, see Fig. 1. This “Neutral Fiber” zone protects the fragile PV cells from external stress such as snow or wind loads, or vibrations during transport that may cause cell breakage, a defect known as microcracks [18]. The combination of a large mechanical strength and a neutral fiber zone for the PV cells, make glass-glass modules very resilient to microcracks. It is expected that microcracks in the PV cells do not arise during transportation, installation, or operation of a glass-glass PV module, even when subjected to high external loads or careless handling of the PV modules [11].

While there are no technical disadvantages to glass-glass PV modules [10,19], in general glass-glass PV designs are more expensive than regular GBS modules due to the use of an additional costly glass layer and the increased weight that may lead to higher costs for support structures. However, the increased costs are supposedly compensated with increased efficiency (when using bifacial PV cells) and enhanced reliability.

### 2.2. Glass characteristics

Glass-glass PV modules generally use 2–3 mm thick glass layers, since thicker glass layers negatively impact the module’s weight and costs, while trends are to reduce glass thickness to below 2 mm [10]. Laminated glass has a higher mechanical strength than monolithic glass, which enables the usage of heat strengthened glass instead of tempered glass. In case laminated glass breaks, the broken shards remain connected to the interlayers [20]. The bonding properties of the interlayers make that laminated glass, and thus glass-glass PV modules, can still provide compressive strength. However, the tensile strength is no longer present. The strength of laminated glass post-breakage is determined by the materials properties of the interlayer, i.e., strength, stiffness, thickness and adhesion level with the glass [20]. In glass-glass PV modules the interlayer is often Polyolefin Elastomer (POE) encapsulant. Subsequent weathering of the encapsulant, such as the ingress of moisture, may decrease the strength of defected glass PV modules. This will reduce

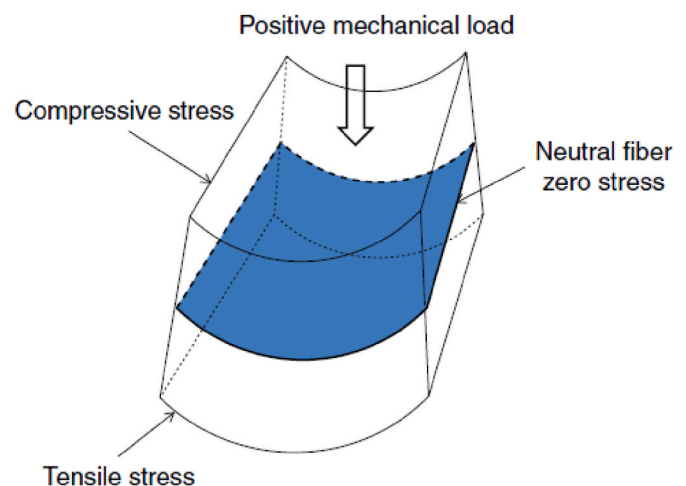


Fig. 1. Schematic overview of the “Neutral Fiber” zone (from Verlinden [11]).

the lifetime of the module and cause corrosion of internal components [20].

### 2.3. Glass defects in PV modules

Glass defects in PV modules refer to cracked or broken glass layers that are caused by human factors or extreme weather such as hailstorms and high wind- or snow loads [21]. The majority of the glass defects arise due to human force during installation, maintenance and primarily during on-site transportation of the PV modules [22]. Glass defects are identified as one of key failures at PV modules, together with delamination, discoloration and junction box (J-box) and cable defects [7,12,13,23–27]. The relative amount of glass defects ranges from several percent up to one of the most prominent failures of registered PV failures. A customer complaints research, on PV modules after two years of operation, observed glass breakage for 10% of the failure cases [28]. Another study on PV failures observed an even higher failure-share for glass breakage. Glass breakage was responsible for 33% of the PV failures, after eight years of operation [29]. Unfortunately, research on PV (glass) failures is mainly focused on regular GBS modules. An extensive literature analysis and review on PV field reliability observed a shift in the significance of failure types over the full time period of the research (early 1980s–2015) and the last ten years (2005–2015). During the last ten years, critical PV failures shifted to hot spots, discoloration and glass breakage (see Table 1). The shift was initiated by the introduction of new PV production techniques and module designs. The importance and frequency of failures will change again with the development of new modules [24], and it is stated that “there is a risk that the change in module construction could result in increased failure rates for different failure mechanisms (e.g., glass breakage for the glass/glass construction)” [30].

#### 2.3.1. Increased importance for glass-glass PV modules

PV failures related to glass-glass PV modules will become more important with increased market share. The structure of glass-glass PV modules enables installation without aluminum frame. The absence of this frame makes that glass-glass PV modules are more prone to glass defects [12]. In frameless glass-glass PV modules, glass defects can contribute tens of percent of the failures in the field, making it the most

important failure for glass-glass PV modules [25,31]. Glass layers break when impacted by stress larger than the inherent glass strength [12]. For PV modules with frames, most glass breakage is caused by direct impact on the glass surface. However, frameless PV modules are sensitive to stress and impact on the glass edge, leading to edge breakage [12,32].

Next to the absence of an aluminum frame, there is the so-called lamination pinch-out at glass-glass PV modules that increases the sensitivity to glass defects. This is very relevant for solar panels in greenhouses, of which numerous large (>5 MWp) projects are (being) build in the Netherlands at the moment. The lamination pinch-out forces the layer sandwich to be thinner at the module edge, therefore bending the front and back layer towards each other [12]. The bending of the front glass layer creates a very high local stress at the module edge. The local stress increases the probability of glass defects significantly, especially in combination with incorrect clamp position, inadequate clamp type or screws [12,31]. However, the majority of glass defects in the case study from Zhang et al. [31] on glass defects in glass-glass PV modules were caused by incorrect handling and maintenance. During on-site handling, the PV modules were knocked or chucked. Incorrect placement mainly caused failures in combination with faulty installation and maintenance [33].

#### 2.3.2. Safety and performance impact due to glass defects

It is not uncommon that defects, failures, and degradation occur in single PV components, while other components and the PV module structure itself remain intact [24]. Glass defects do not necessarily impact the PV module’s performance, since modules with glass cracks may still function correctly over time. For example, Ndiaye et al. [14] documented modules with broken glass that do not show a noticeable power decrease. At the TNO location in Petten, the first back contact PV module is still operating with a broken glass front layer that arose during transportation [34]. However, glass breakage could potentially reduce the direct solar radiation on the solar cell, which (slightly) lowers PV performance [35]. In contrast, Hwang et al. [36], measured drastic power reduction after laboratory tests with broken (glass) PV modules. The glass breakage was inflicted by the application of a large external force on the PV module [35]. Nevertheless, Eder et al. [37] reported no performance decrease after inflicted glass breakage by thermal tension. It is evident that the impact on performance by glass breakage is diverse

**Table 1**  
Overview on PV failure research.

Source	Type of PV modules	Observed PV failures (% of total failures)
Case study on customer complaints [28]	Multiple module types, after two years of operation	Optical failure (20%) Power loss (19%) J-box and cables (19%) <b>Glass breakage (10%)</b>
Extensive field study [29]	Multiple module types, after eight years of operation	Defect interconnections (36%) <b>Glass breakage (33%)</b> J-box and cables (12%)
Review and analysis of PV field reliability [25]	Multiple module types	Occurrence x Severity (scaled to 100%) Encapsulant discoloration (45%) Major delamination (15%) Hot spots (12%)
Review and analysis of PV field reliability [25]	Multiple module types	Occurrence x Severity (scaled to 100%) Hot spots (32%) IC discoloration (19%) <b>Glass breakage (13%)</b>
Review and analysis of PV field reliability [25]	Thin-film double-glass laminated PV modules.	Occurrence x Severity (scaled to 100%) <b>Glass breakage (38%)</b> Absorber discoloration (27%) Minor delamination (15%)
Review of PV failure modes [26]	Silicon PV modules	Delamination (42%) Corrosion (19%) <b>Soiling/Glass breakage (19%)</b>
Review of PV failures in the field [27]	Silicon PV modules in moderate climate zone	Moisture ingress (19%) Snail tracks (12%) Defect back sheet (9%) <b>Glass breakage (7%)</b>

and case specific. Similar variation in PV performance degradation by glass breakage was observed by Jordan et al. [25]. The impact of glass breakage on PV performance spans the full degradation spectrum (scale 1–10), from very severe cases (10) to insignificant effects (1) with an average severity of 5 [25]. PV cell breakage is a likely explanation for the variation in performance directly after glass defects [17].

The impact that caused the glass layer to break can subsequently generate or enhance microcracks. These cell cracks are barely detectable by visual inspection and require optical methods for detection [13]. The power decrease by microcracks can range from negligible power loss, up to severe (5–10%) performance decrease [38]. The impact of microcracks is determined by the PV-cell type (e.g., monocrystalline, polycrystalline) and the size and location (e.g., vertical, busbar, horizontal) of the microcracks [39]. As mentioned before, glass-glass PV modules are very resilient to microcracks. However, scientific literature is not decisive on the formation of microcracks at glass-glass PV modules that suffer glass defects.

The performance degradation of glass breakage is therefore mainly caused by secondary effects and performance degradation occurs in steps over time until saturation [12]. The degradation seen in PV modules with glass defects is generally initiated by the ingress of water. Water (vapor) that gains access to the active components of the PV module can cause various issues that can divert the path of the current in the PV module, creating stray currents that cause power loss. Another type of degradation due to water ingress is the corrosion of the PV module, in particular the corrosion of PV cells and the discoloring of the encapsulant film [11]. Next to these two examples, there are several other degradation types related to the ingress of water, such as “snail tracks”, discoloration and humidity-freeze conditions [11]. The subsequent degradations that might occur at broken glass PV modules, stress the importance of glass layers as proper water barrier.

The glass layers insulate and protect the encapsulant and PV cells from the environment, in particular from humidity. A major problem is that electrical safety is no longer guaranteed when moisture is able to penetrate to the live parts of the PV module. Wet conditions impact the insulation of the PV module and might cause electrical shocks or even fire [12]. Another safety issue is the generation of hot-spots, these occur when the operating current exceeds the short-circuit current of a(n) inactive/low-active cells and create localized heating [40]. Inactivity of cells may be caused by microcracks or partial shading, the heat at these hot spots can cause electrical and fire problems [12]. The probability of (in)direct degradation and electrical shocks by glass defects, make that PV modules with glass defects do not meet the safety and performance standards set by the International Electrotechnical Commission (IEC 61215 and IEC 61730) [41] (see Appendix A for more details). The reparation of the insulating glass layers should aim to restore the reliability, in terms of safety and performance, of the PV modules.

### 2.3.3. Economic impact of glass defects

Glass defects impact the economic performance of a PV system in multiple ways. The most obvious effect is the potential (in)direct performance loss of PV modules, which results in reduced economic revenues. Secondly, PV modules that suffer from glass defects may no longer meet safety requirements, therefore these modules are replaced. Research by Moser et al. [42] analyzed the economic impact of PV failures with a failure mode and effect analysis (FMEA). We refer the reader to their paper, for further background information and assumptions. The economic impact of glass breakage was calculated using a cost priority number (CPN), and the costs of glass breakage was calculated at 8.5€/kWp/year. We note that glass breakage is the second most costly failure after improper installment of PV modules, which is 13€/kWp/year [42].

### 2.4. Case study

The case study is a PV project from SolSolutions, a solar-energy

company that is actively developing new solar applications for the agricultural sector. The case study is a project at a large garden center in the Netherlands, which uses an empty greenhouse as storage. The requirement for light transmission and the existing structure made this a technically challenging project. Therefore, the case study made use of custom-made PV modules developed by DMEGC Solar and SolSolutions [43]. The PV modules have three distinctive characteristics: double glass for light passage, bifacial PV cells and extra thin glass (1.6 mm per layer). The PV installation entails 4236 PV modules in strings of 24 PV modules [44]. The usage of extra-thin glass enhanced the occurrence of glass (edge) breakage. The total number of double glass PV modules with glass defects was 43, of which 30 PV modules were directly removed. There are currently about 13 PV modules operating with (minor) glass defects, and these have not shown any reduced performance or other degradation [44]. The directly removed PV modules were stored in dry conditions in a standard transportation containment, of which four specimens were selected with glass defects at the back layer for our study, that included experiments based on various part in the appropriate IEC standards, such as damp heat tests.

## 3. Materials, specimen, and methods

### 3.1. Specimen

A sample set of six specimen was used for this research, divided into two distinctive groups: as-received glass-glass PV modules and glass-glass PV modules with glass defects. The glass defects all arose during transportation and installation. PV modules with glass defects were directly removed and stored in an appropriate container, protected from the environment but exposed to indirect irradiance. The selected glass defect specimen endured defects at the back glass layer, average damage, edge pits and suffered from no other visual defects. The as-received glass-glass PV modules did not show any visible deficiencies and were used as reference during the test series. After the initial tests, the glass defect PV modules were divided into two subgroups: repaired specimen and non-repaired specimen. The repaired specimen were treated with the experimental repair technique, whereas the non-repaired specimen were left untreated as reference. Therefore, the research specimen consist of the following configurations:

Glass defect specimen.

- Repaired PV specimen (RP) - experimental repair technique (specimen 1 and 4).
- Non-repaired PV specimen (NR) – left untreated (specimen 2 and 3).

As-received (AR) specimen.

- Reference specimen as received from the manufacturer that did not show any deficiencies (specimen 5 and 6).

**Table 2**  
Specifications of the specimen used.

Module details		Performance specifications	
Dimensions (length x width x height)	1649 x 996 × 4.2 mm	Maximum Rating Power (Pmax)	290 W
Cell Type	Mono Crystalline (PERC)	Module Efficiency	17.66%
Cell Arrangement	54 (6 x 9)	Open Circuit Voltage (Voc)	35.96 V
Application Class	Class A at IEC 61730	Voltage Maximum Power Point (Vmpp)	30.17 V
Weight	15.7 kg	Short Circuit Current (Isc)	10.02 A
Maximum Load Capacity	Snow 2400 Pa/ Wind 2400 Pa	Current Maximum Power Point (Impp)	9.62 A
Cell Encapsulant	PolyOlefin Encapsulant (POE)		



**Table 3**  
Experimental glass reparation using UV-curing resin.

Step	Description
Step 1: Inspection of the glass fracture	<ul style="list-style-type: none"> <li>• Determine freshness of the fracture (old fractures might contain dirt)</li> <li>• Determine the end of the fracture.</li> </ul>
Step 2: Temperature of the PV module	<ul style="list-style-type: none"> <li>• During the reparation the temperature of the PV module should remain between 5 °C and 29 °C. The glass temperature is optimal at 20 °C.</li> <li>• Cool or heat the PV module to the required temperature.</li> <li>• Check for presence of water. In case the fracture contains water, heat the module to evaporate the water. This can be done locally with a heat gun or in a heated room or enclosure.</li> </ul>
Step 3: Preparing the fracture	<ul style="list-style-type: none"> <li>• Place the module horizontal with the fractured glass surface upward.</li> <li>• Clean the module with window cleaner, brand name Glassex, to remove the surface from any dirt or grease.</li> </ul>
Step 4: Applying the repair resin.	<ul style="list-style-type: none"> <li>• Insert the repair resin into the fractures using small drops.</li> <li>• Steadily go along the fractures with the repair resin while applying a small paintbrush onto and into the fracture</li> <li>• Check if the resin is flowing into the fracture. If the resin is not flowing into the fracture, then slowly vibrate the module near the fracture in a controlled manner</li> </ul>
Step 5: Applying the pit resin.	<ul style="list-style-type: none"> <li>• Remove the surplus resin with dry and lint-free paper.</li> <li>• Apply drops of pit resin on top of the larger edge pits.</li> <li>• Apply the pit resin on top of the fractures as a top sealant, do not use the small paintbrush.</li> <li>• Check if all fractures and pits are sufficiently covered with pit resin.</li> </ul>
Step 6: Curing the repair and pit resin.	<ul style="list-style-type: none"> <li>• Place the UV lamp at a distance of 20–30 cm and cure for a minimum of 20 min.</li> <li>• Or place the PV module horizontally facing the sunlight (radiant day) for a minimum of 30 min.</li> </ul>
Step 7: Finishing the reparation	<ul style="list-style-type: none"> <li>• Check if all fractures are repaired.</li> <li>• Clean the PV module using demineralized water.</li> </ul>

The specimen used for this study were customized glass-glass PV modules designed for greenhouses and therefore had unique dimensions. In order to fit the PV modules into the existing greenhouse, the specimen required a thickness of 4.2 mm, existing out of two identical glass layers of 1.6 mm each and intermediate layer of cell encapsulant and PV cells of 1 mm thick. The specimen were made with monocrystalline PERC PV cells (c-Si), polyolefin encapsulant (POE) and semi-tempered glass. The application of PERC PV cells made the glass-glass PV modules bifacial, the rear side output was not included into the module's power rating [45]. All specimen met the IEC 61215 and 61,730 standards upon fabrication. The module and electrical specifications are available in Table 2.

### 3.2. Experimental repair technique

The experimental repair technique for glass defects at double-glass PV modules was based on a method for edge pit reparation at windshields from NOVUS [46] and the experience from Falk [47] and its seven steps are detailed in Table 3.

The materials required for the experimental reparation consists out of repair resin and pit resin designated for windshields that aim to restore the strength and insulation of the glass layer(s). Furthermore, an UV lamp with an intensity of 108 W UVA is required for the strengthening of the resin, the resin can also be cured by natural UV light. All other materials were supplementary but improved the quality of the reparation.

### 3.3. Visual inspection

The most common and straightforward method to determine the quality and reliability of a PV module is visual inspection. Visual inspection consists out of a systematic check and does not require any testing devices but should be conducted at  $\geq 1000$  lux illumination for appropriate assessment [47]. The method can detect failures before (time) expensive techniques are introduced. Therefore, all PV modules in the IEC standards are first subject to the visual inspection [42]. Our research applied the method for visual inspection of PV modules introduced by IEA-PVPS [12].

### 3.4. Electroluminescence test

In the electroluminescence (EL) test, a power supply source forces a current through the PV module, which initiates EL emission from the PV

cells. A charge-coupled device (CCD) or complementary metal-oxide-semiconductor (CMOS) camera can capture these EL radiations and convert these to images [48]. Internal failures appear as black/dark spots and show that these live PV parts are inactive. Trained experts and computer modules can distinguish internal failures from these EL images, which makes the test valuable for defect detection at cell levels that are not noticeable during visual inspection. Potential PV failures that may be obtained from EL images are inactive cells, microcracks, shunts, among many others [49].

### 3.5. Current-voltage test

The principal purpose of a PV module is to convert photon energy into useable power (electricity), the performance can be measured with the current-voltage (IV) test. The IV test measures variation of current and voltage under specific conditions and from the IV characteristics parameters such as short-circuit current ( $I_{sc}$ ), open-circuit voltage ( $V_{oc}$ ), fill factor (FF), and maximum power point ( $P_{max}$ ) can be derived. The IV characteristics are cross-referenced with IV curves from the manufacturer and reference modules. Differences in measured IV indicators imply that the PV modules may suffer from malfunctions.

### 3.6. Accelerated lifetime test

The reliability and durability of PV modules are of great importance in the PV sector. Therefore, the module's capability to withstand accelerated lifetime tests is imperative [50]. The damp-heat (DH) test method is an integral method that verifies the PV module's ability to endure long-term exposure to humidity penetration [30]. Therefore, DH is part of the MQT and MST sequences of the IEC 61215 and 61,730 standards. A certified DH test should be carried out in accordance with the IEC 60068-2-78, which is a separate DH test standard [41].

In the DH test the PV modules are mounted in an enclosed climate chamber that is capable of maintaining a temperature with 1 °C degree accuracy and is regulated with an automatic control system. The specimen are subject to 1000 h of test duration during which the climate chamber is constantly kept at 85 °C ( $\pm 2$  °C) and relative humidity of 85% ( $\pm 5\%$ ). The PV modules are fitted with temperature sensors to monitor the module's ability to withstand extreme conditions [42]. The IEC 61215 requirements to pass the DH test are.

- a) No evidence of major visual defects\*

- b) Degradation of maximum output power shall not exceed 5% of the value measured.
- c) Insulation resistance still meets the initial measurements.
- \* excl. repaired glass defects in this research

The damp-heat test can identify several potential PV failures caused by the penetration of moisture [30]. However, the humidity levels in the DH test are higher than will ever be experienced in field operation [30]. A successful DH test ensures that a (repaired) PV module is capable of enduring humidity ingress for long-term field operation.

### 3.7. Degradation rate calculation

The degradation rate (DR) is an important parameter for PV lifetime and performance. The DR is calculated based on test results, however some problems that arise during the accelerated lifetime tests may never occur in real conditions [14]. The DR is sensitive to the testing conditions and methods that are used for calculation. This research applied a compound DR formula based on the performance results (maximum power) after the DH test ( $P_{DH}$ ). The lifetime equivalent of the DH test was set at 30 years, based on the research by Wohlgemuth [30] that concluded that long-term operating PV modules will never experience such humidity levels. The 30 years were also used by Ref. [43] for their performance warranty. The DR is an annual degradation that has a negative value, which is calculated for the PV specimen using the following formula:

$$DR = \left( \sqrt[30]{\frac{P_{DH}}{P_{module}}} - 1 \right) \times 100\% \tag{1}$$

in which  $P_{DH}$  is  $P_{max}$  after DH test (in W),  $P_{module}$  is the label capacity (290 W) and lifetime  $t$  (in years) is 30 years [43].

### 3.8. Economic impact indicators

A good understanding of technical risks (PV failures) and the associated costs is crucial for the development into a mature market [42]. Failures impact the power output of the PV system and thus the economic performance. Prevention, reparation and substitution of PV failures each have an economic impact. Therefore, this research analyzed the economic impact of glass reparation using several economic indicators for five different scenarios, see Table 4. Base scenario 1 (BS1) reflects the situation in which defect modules are uninstalled and substituted. Base scenario 2 (BS2) substitutes the defect PV modules that break during installation directly, therefore uninstallation is not required. Reparation scenario 1 (RS1) uninstalls the defect modules, repairs and conducts performance and reliability tests. Reparation scenario 2 (RS2) repairs installed defect PV modules in-situ, without performing additional performance tests. Reparation scenario 3 (RS3) repairs the PV modules directly in-situ and conducts performance and reliability tests.

#### 3.8.1. Failure mode and effect analysis

The failure mode and effect analysis (FMEA) is an effective method to

**Table 4**  
Fixture scenarios for economic analysis.

Scenario	Description	Abbreviation
Base Scenario 1	Substitution of the defect PV modules	BS1
Base Scenario 2	Direct substitution of the defect PV modules	BS2
Reparation Scenario 1	Reparation of the defect PV modules, incl. uninstallation and testing	RS1
Reparation Scenario 2	In-situ reparation of the defect PV modules	RS2
Reparation Scenario 3	Direct reparation of the defect PV modules with testing	RS3

**Table 5**  
Description of the parameters in the CPN and CPN/kWp calculations.

Parameter	Description	Value or equation	Unit	Source
CPN	Cost Priority Number	Eq. (B1)	€/year	[42]
CPN/kWp	Cost Priority Number per kilowatt peak	Eq. (B2)	CPN/kWp	[42]
$C_{down}$	Cost of downtime	Eq. (2)	€	Derived from [42]
$C_{fix}$	Cost of fix	Eq. (3)	€	[42]
L	Production losses during downtime	Eq. (B3)	kWh	[42]
SDE	Subsidie Duurzame Energie (SDE)	0.079	€/kWh	[51]
$C_{dec}$	Cost of failure detection	0	€	[42]
$C_{sub}$	Cost of failure substitution	90–95	€/per module	Case study data [44]
$C_{rep}$	Cost of reparation	Eq. (4)	€	
$C_{trans}$	Cost of transport	10	€	[42]
$C_{lab}$	Cost of labor	50–60	€/h	[44]
$C_{mat}$	Cost of materials	15–30	€	[44]
$C_{test}$	Cost of testing repaired PV modules	20	€	[52,53]
$N_{fail}$	Number of failures	43		Case study data [44]
$N_{comp}$	Number of PV modules in the system	4235		Case study data [44]
$N_{fail, year}$	Number of failures (affected components/year)	Eq. (B4)		[42]
$T_{down, fail}$	Downtime due to failure	Eq. (B5)	hours	[42]
$T_{down}$	Downtime in total	Eq. (B6)	hours	[42]
$T_{down, comp}$	Downtime due to failure – normalized by total number of components	Eq. (B7)	hours	[42]
$O_{CPN}$	Occurrence	Eq. (B8)		[42]
$S_{CPN}$	Severity	Eq. (B9)		[42]
$W_{module}$	Label wattage module	290	W	[43]
$T_{fix}$	Time to fix the failure (h)	Base scenario 1 Base scenario 2 Reparation Scenario 1 Reparation Scenario 2 Reparation Scenario 3	1.75–2.25 0.5–1.0 2.5–3 1–1.5 1–1.5	hours [42,47]
PL	Performance Loss (%)	10–50	%	[42]
$T_{tr/ts}$	Time between detection and reparation (h)	744	hour	[42]
$T_{dec}$	Time before detection	8760	hour	[42]

(continued on next page)

**Table 5** (continued)

Parameter	Description	Value or equation	Unit	Source
$T_{ref}$	Performance reduction over whole portfolio per year (h/year)	1000	Full load hours	[54]
M	Multiplier	1–3		[55]

**Table 6**

Variety in the input variables for the sensitivity analysis.

Variable	Abbreviation	Range	Unit
Time to fix	$T_{fix}$	0.5–3	hours
Costs of product	$C_{prod}$	15–95	€
Cost of labor	$C_{lab}$	50–60	€
Multiplier	M	1–3	
Performance loss	PL	10–50	%

create insight into risks and enables the management of these risks. Moser et al. [42] introduced the FMEA to the PV industry and incorporated the cost priority number (CPN) for the analysis of economic impacts from PV failures. The CPN/kWp is a derivative of the CPN and makes the impact comprehensible and comparable. The method from Moser et al. [42] was modified in this research for several indicators. One of the adjustments is the substitution of parameters: feed-in-tariff, power purchasing agreements and retail costs for electricity (FIT, PPA and RCE, respectively) by one single input parameter specific for the Dutch situation, named ‘Subsidy for Sustainable Energy’ (SDE) [51].

$$C_{down} = L \times SDE \tag{2}$$

This adjustment was made for simplicity and coherence with other case-specific data. Another modification is the addition of the variable repair costs.

$$C_{fix} = (C_{dec} + C_{rep\ or\ sub} + C_{transp}) \times n_{fail} + C_{lab} \times t_{fix} \times n_{fail} \tag{3}$$

$$C_{rep} = C_{mat} + C_{test} \tag{4}$$

The FMEA was calculated for case specific data. The modifications on the method from Moser et al. [42] led to the final equations (Eq. B1–B9, see Appendix B) that were calculated using the parameters in Table 5 and Table 6 (sensitivity analysis).

### 3.8.2. Sensitivity analysis on FMEA

Sensitivity analyses determine which parameters are most influential in the uncertainty of the model’s outcome [56]. The application of an experimental technique is surrounded by (practical) uncertainties. To overcome these uncertainties, the research applied a scenario with

**Table 7**

Description of the parameters in the NPV and PBT calculations.

Parameter	Description	Value or equation	Unit	Source
NPV	NPV	Eq. (5)	€	[59]
PBT	Payback Time	Eq. (6)	years	Derived from [59]
$CF_t$	Cash Flow	Eq. (7)	€	Derived from [59]
CPN	Cost Priority Number per scenario	CPN calculations	€	
R	Discount Rate	1.5	%	[54]
SDE	Subsidie Duurzame Energie	0.079	€/kWh	[51]
PR	Performance Ratio	0.85		[60]
FLH	Full Load Hours	1000	hours	[54]
E	Annual Electricity production to the grid	Eq. (8)	kWh/year	
$W_{module}$	Label wattage module	290	W	[43]
D	Annual degradation per module	DR calculations	%	
T	Time	$T_{new} = 15$ $T_{rep} = 15$ $T_{no-rep} = 15$	years	[51]

different repair and substitution prospects. To analyze for important input parameters, a ‘global’ sensitivity analysis was conducted including a large range of uncertainty from all scenarios, see Table 6. The method applied in this research is the Sobol Sensitivity Analysis, which is suitable for ‘global’ analysis regarding multiple input uncertainties [57]. We used the implementation in Python [58].

### 3.8.3. Net present value and economic payback time

The Net Present Value (NPV) is one of the most widely applied indicators for economic decisions. The future economic returns are discounted into a present value, which indicates if an investment is profitable or not. Another useful economic indicator is the economic payback time (PBT): the period it takes to pay back the initial investment costs for substitution or repair. The timeline for the NPV and PBT calculation was based on the subsidy period (15 years). The NPV and PBT equations (5)–(8) are based on the equations from Ebrahimi & Keshavarz [59] with an added correction for inflation using a discount rate. Data are given in Table 7.

$$NPV = \sum_{t=0}^n \frac{CF_t}{(1+r)^t} - CPN \tag{5}$$

$$PBT = \sum_{t=0}^n \frac{CF_t}{(1+r)^t} = CPN \tag{6}$$

$$CF_t = SDE \times E \tag{7}$$

$$E = (W_{module} \times D \times (t-1)) \times FLH \times PR \tag{8}$$

### 3.9. Net energy analysis

PV modules convert photon energy into useable electricity without any operational fuels. However, PV modules require energy investments along the supply chain, e.g., resource extraction, manufacturing, transportation, installation, and decommissioning [61]. Therefore, not all generated electricity is directly adding to a positive energy surplus. To quantify the effectiveness of the PV module performance there are several indicators for net energy analysis (NEA). This research defined three scenarios for the NEA: 1) repair, 2) do-nothing alternative, and 3) substitution of glass defects. Each scenario has different invested energy inputs and expected energy generation. Net energy analysis is valuable for a well-substantiated energy trade-off.

In this research, we calculated the energy payback time (EPBT), the energy return on investment (EROI) and the net energy gain (NEG) based on [61,62]. The EROI calculates the ratio of total electricity output over the PV module’s lifetime to the sum of required energy investment per module. A large  $EROI_{PE-eq} > 1$  (with PE-eq primary energy equivalent) implies that the PV module is adequately contributing energy to the energy system instead of demanding energy. As a

**Table 8**  
Description of the parameters in the NEA calculations.

Parameter	Description	Value or equation	Unit	Source
EPBT	Energy Payback Time	Eq. (9)	Years	[61,62]
EROI	Energy Return on Investment	Eq. (10)		[61,62]
NEG	Net Energy Gain	Eq. (11)	kWh	[61,62]
Out <sub>el</sub>	Total energy output over PV module lifetime	Eq. (12)	kWh	Derived from [59,63]
Out <sub>PE-eq</sub>	Energy delivered to the society	Eq. (13)	kWh	[61,62]
Inv	Invested energy in PV module	3550 5.45	MJ/m <sup>2</sup> MJ/reparation	[63]
η <sub>g</sub>	Energy efficiency of electricity grid	30	%	[63]
W <sub>module</sub>	Peak wattage module	290	W	[43]
PR	Performance Ratio	0.85		[60]
FLH	Full load hours	1000	hours	[54]
D	Degradation	DR calculations	%	
T	Time	T <sub>new</sub> = 15, 25 and 30 T <sub>rep</sub> = 15, 25 and 30 T <sub>no-rep</sub> = 15, 25 and 30	years	

consequence, the NEG is positive (NEG >0) and the PV module is not demanding energy from the energy system.

The invested energy in the PV specimens (Inv) was calculated using the Life Cycle Analysis (LCA) software SimaPro 9, which supports cumulative energy demand (CED) calculations. SimaPro holds several major LCA libraries of which Ecoinvent v3 was utilized, the Inv was calculated using the CED v1.11 calculation set-up [54]. In accordance with Fthenakis & Leccisi [60] this research applied an average grid efficiency (η<sub>g</sub>) of 30% and PV performance ratio (PR) of 0.85. The generalized grid efficiency is coherent with an energy mix that is dominated by conventional fossil-based electricity generation technologies. PV system losses (e.g., DC-AC conversion, cable resistance) are all accounted for in the PR. Data are given in Table 8 and used equations are:

$$EPBT = Out_{el} / \eta_g = Inv \tag{9}$$

$$EROI_{PE-eq} = \frac{Out_{el} / \eta_g}{Inv} \tag{10}$$

$$NEG = Out_{PE-eq} - Inv \tag{11}$$

$$Out_{el} = \sum_{t=0}^{t=i} W_{module} \times D_x^t \times FLH \times PR \tag{12}$$

$$Out_{PE-eq} = Out_{el} / \eta_g \tag{13}$$

**Table 9**  
Summarized results from the visual inspections at each research phase.

Research specimen	Initial inspection	After reparation	After damp-heat exposure
Specimen #1 (RP)	Glass defects: edge pit and multiple (large) cracks at back layer	No visual changes	Discoloration (brown) of the pit resin at the edge pit and cracks
Specimen #2 (NR)	Glass defects: edge pit and multiple (medium) cracks at back layer	n.a.	Multiple additional large cracks over the full PV module width at back layer
Specimen #3 (NR)	Glass defects: edge pit, multiple (large) cracks at back layer	n.a.	No visual changes
Specimen #4 (RP)	Glass defects: two minor edge pits, multiple (small/medium) cracks at back layer	No visual changes	Discoloration (brown) of the pit resin at edge pit locations
Specimen #5 (AR)	No visual defects	n.a.	No visual changes
Specimen #6 (AR)	No visual defects	n.a.	No visual changes

## 4. Results and discussion

### 4.1. Visual inspection and internal inspection

The specimens with glass defects did not endure any other defects than glass defects at the initial inspection, therefore defects in subsequent research phases were ascribed to the reparation process or the DH test. The AR specimens had no visual defects at the start of the research. At the initial inspection all research specimens were internally analyzed using EL images. None of the PV modules showed visible irregularities, which indicates that the impact on the edge causes the glass layer to break but does not directly place the PV cells under stress. This confirms the expectations from Verlinden [11] that double-glass PV modules are resilient to microcracks. After the reparation, the RP specimens were once more visually inspected, and the results show that the reparation process did not inflict any additional visual defects, neither did the EL images show any internal deformities. Therefore, we conclude that the repair process itself does not negatively impact the PV module. An overview of results can be seen in Table 9.

After the DH test, a visual change was registered at three specimens. The RP specimens endured discoloration of the pit resin. The combination of high temperature and extreme humidity, which “boil” the pit resin, is the presumed cause for color change [47]. However, discoloration of pit resin does not impact the quality of the resin [47]. Specimen RP did not show any additional glass defects or crack extensions. Next to this, the absence of signs of water (e.g., trapped moisture, corrosion or delamination) indicate that the reparation succeeded in restoring the glass layer as an insulator.

The third specimen with visible change was specimen 2 (NR), at which multiple large glass cracks were added to the existing glass defects. The additional cracks are ascribed to the weathering of the PV



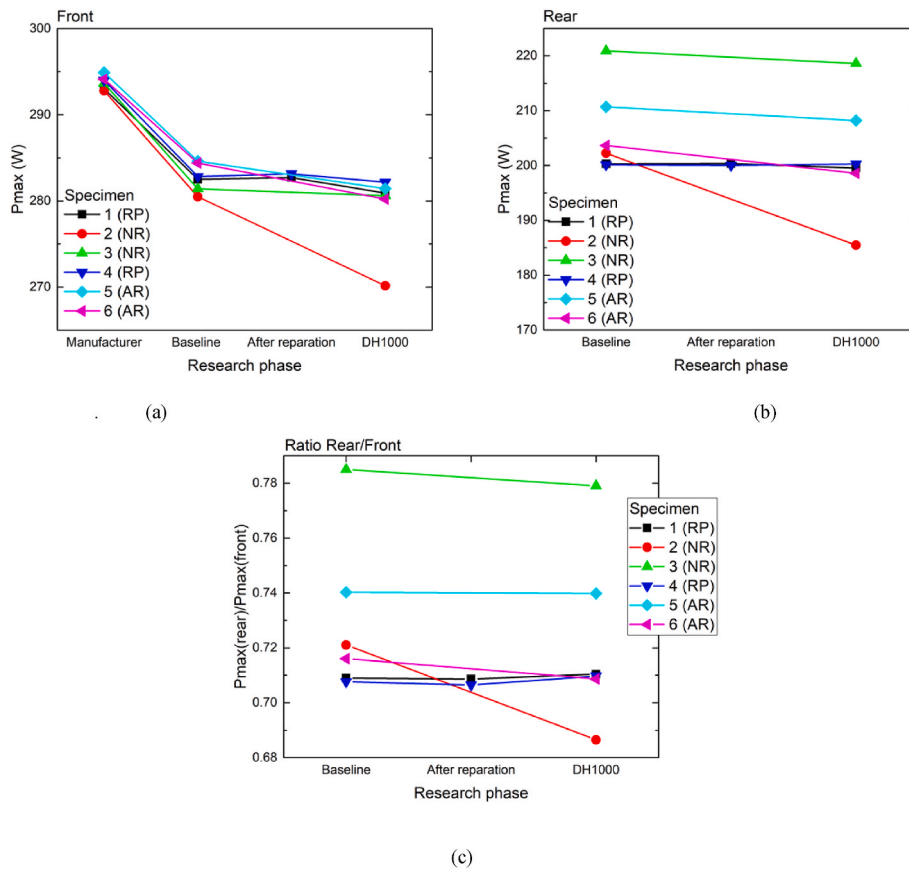


Fig. 2. Measured maximum power  $P_{max}$  (W) of the various PV modulea at each phase of the research phase, (a) front side, (b) rear side, and (c) power ratio of rear to front side. The black and dark blue lines (specimens 1 and 4), represent the repaired PV modules. The read and green lines (specimen 2 and 3), the non-repaired PV modules, and the light blue and purple lines (specimen 5 and 6), are the as-received (reference) PV modules.

module by the DH test. The EL images confirm the degradation at specimen 2 and denote significant PV cell degradation (see Appendix C). However, specimen 2 did not register any visible indications for water infiltration. Research by Yang et al. [64] identified that POE encapsulant has a low WVTR at frameless double-glass PV modules, this could have constrained the visible water ingress. The other three specimen (specimen 3, 5 and 6) did not register any visible change. Degradation is inherent to DH testing, the EL images from these three specimen showed gradual change in grayscale, indicating an uniform degradation of the PV cells.

#### 4.2. Change in performance

The first IV measurements were performed by the manufacturer and show a performance decrease between the fabrication (May 2020) and the baseline tests (March 2021), from 292 to 295 Wp to 280–285 Wp (or about 3–4% decrease). During this period, the PV modules were shipped to the Netherlands, but more importantly exposed to solar irradiance at the location of their installation. The exposure to solar irradiance causes PV modules to slightly degrade due to light-induced degradation (LID) [65]. These degradation types are generally accepted when limited to

3% degradation of the rated capacity and are included in the product sheet of the manufacturer [43]. Another explanation for the measured performance decrease is the difference in test setup. Both test setups use conditions based on to the IEC standards, however differences will always remain [43,66]. All research specimen remained within the acceptable range, even though specimens 1–4 additionally endured glass defects. The specimen RP and NR that suffered from glass defects show a

Table 10  
Degradation rates based on DH test results.

Category	Degradation rate (DR) (t = 30 years)	Estimated Experimental Error (%)
Reference	0.10%/annually	83%
Repaired	0.10%/annually	83%
Non-repaired	0.17%/annually	72%

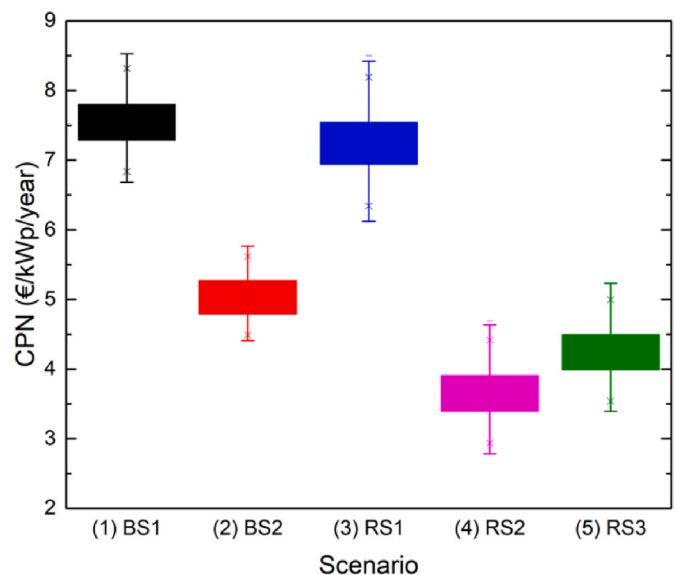


Fig. 3. CPN value distributions of each fixture scenario (€/kWp/year).

slightly lower rated capacity at the baseline, however this difference is insignificant and may be contributed to the longer exposure to solar irradiance.

The reparation did not negatively impact the performance of the RP specimens and even showed a small increase in module performance. The final measurements after the DH test show very similar performance outputs for five out of six specimen. The exception is specimen 2 (NR) with a significant decrease in performance (7.8% decrease compared to the manufacturer measurements). Therefore, specimen 2 does not comply with the IEC 61215 standards for DH testing. The IV-curves after the DH test show no irregularities but there is a decrease in mainly  $I_{sc}$  and  $I_{mpp}$  (see Appendix D, Fig. D1 for the plotted data, including  $V_{oc}$ ,  $V_{mpp}$ , and  $FF$ ).

The other NP specimen (specimen 3) shows performance within a close range with the RP and AR specimens. These five specimens have rated capacities in between 280 and 283 W after the DH test, see Fig. 2. This translates to a performance decrease of 4.0%–4.7% compared to the manufacturer. These results are all within the <5% performance decrease range, set by the IEC standards [48]. However, IEC standard 61,215 is applied to newly fabricated PV modules at which no LID occurred. In this research the LID is included. Therefore, the initial measurements are the most sensible reference and make that all specimen pass the IEC 61215 test. It is interesting to note that the ratio of rear-to-front power (bifaciality factor) differs up to about 10% between the modules. An interesting observation is the high rearside performance of specimen 3, which cannot be explained by the conducted tests. The non-repaired panel specimen 2 shows a reduction in power for both the front and rearside, while also the bifaciality factor decreases. This specimen had multiple additional large cracks at the back layer, which apparently cause this, as the other non-repaired panel specimen 3 did not show this reduction in power.

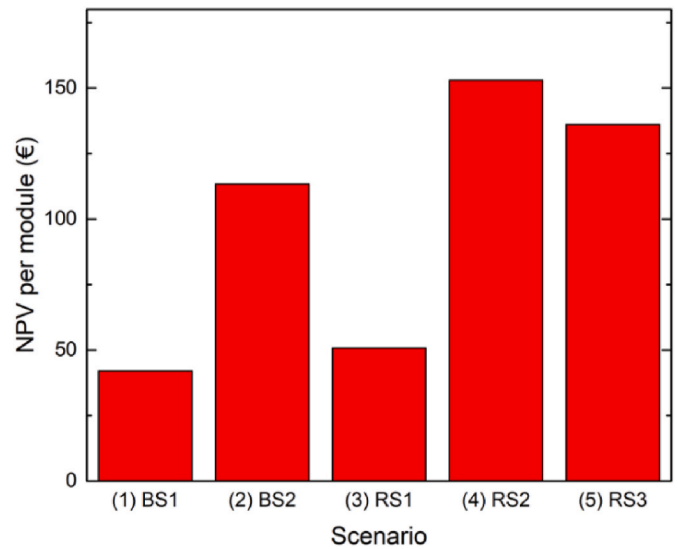
#### 4.3. Degradation rates

The DR set by the manufacturer is 0.6%/annually, with a performance warranty of no less than 82.25% of the label capacity after 30 years [43]. The degradation rates calculated from the measured data by this research are considerably lower than the DR set by the manufacturer, see Table 10. The difference originates from the method and aim that were used in the calculation. The manufacturer based the calculation on the cumulative degradation of all accelerated lifetime tests, next to this it is likely that a surplus degradation was added to prevent warranty claims. Furthermore, various formulas can be applied for the DR calculation [13]. This research calculated the DR on the results from a singular accelerated lifetime (Damp Heat) test and does not include warranty issues for obvious reasons. The DH test is an accelerated lifetime test that exposes the PV modules to more humidity than PV modules would experience in field exposure [30]. However, during complete MQT and MST series and field operation, the PV modules are subject to a much wider range of degrading conditions, which may result in a higher cumulative DR.

**Table 11**

Results from the Sobol sensitivity analysis on the input variables for the CPN of PV modules with glass defects. The table gives an overview of direct influence (first order indices) per variable and the total influence (total order indices) per variable. The confidence interval gives the range at which 95% of the influence distribution on the CPN per variable was calculated.

Variables	First order indices (ST1)	Confidence interval (95%)	Total order indices (ST)	Confidence interval (95%)
Costs of products	0.250	0.040	0.250	0.019
Time to fix	0.754	0.066	0.752	0.053
Labor costs	0.011	0.0106	0.014	0.0015
Performance loss	0.00057	0.0021	0.00068	6.74114e-05
Multiplier	0.00043	0.0019	0.00043	3.84205e-05



**Fig. 4.** NPV per module of each fixture scenario (in €).

#### 4.4. Economic perspectives

Fig. 3 shows the CPN/kWp for each fixture scenario, as defined in Table 4, based on information from the case study. The boxes show the results from the ranges within that scenario, the graph shows that there are significant differences among the scenarios. Scenario (4), RS2 (in-situ reparation of the defect PV modules) has an average CPN/kWp of 3.65 €, making it the least expensive option for glass defects of installed PV modules and the least expensive option overall. The other two scenarios, RS1 (Reparation of the defect PV modules, incl. uninstallation and testing) and BS1 (Substitution of the defect PV modules) are expected to be significantly costlier with 7.24€ and 7.55€ per kWp/year, respectively. The cost difference is caused by the required time to repair or substitute the defective PV module. Scenario RS2 assumes an in-situ reparation of the glass defects and therefore uninstallation is not necessary, subsequently tests are not possible. The RS2 fixture scenario is the least comprehensive and therefore the cheapest option for glass defect fixtures.

The low required costs for scenario RS2 correspond with the results from the sensitivity analysis, which shows that ‘time to fix’ is the most dominant parameter to the output, see Table 11. The variance in CPN outcome is for 75% influenced by the ‘time to fix’ variable, followed by ‘costs for products’ with 25% influence. The reparation method for glass defects makes use of relatively inexpensive materials compared to the substitution of a PV module. However, the reparation requires substantially more time than substitution and thereby reduces the economic impact. Standardization may improve the time efficiency of the repair technique. The costs for testing and materials likely decrease when reparation is applied on larger scale.

To repair or substitute glass defects of installed PV modules with more assurance, the application of scenario BS1 or RS1 are alternatives. In the repair scenario RS1 the PV module is uninstalled, repaired and

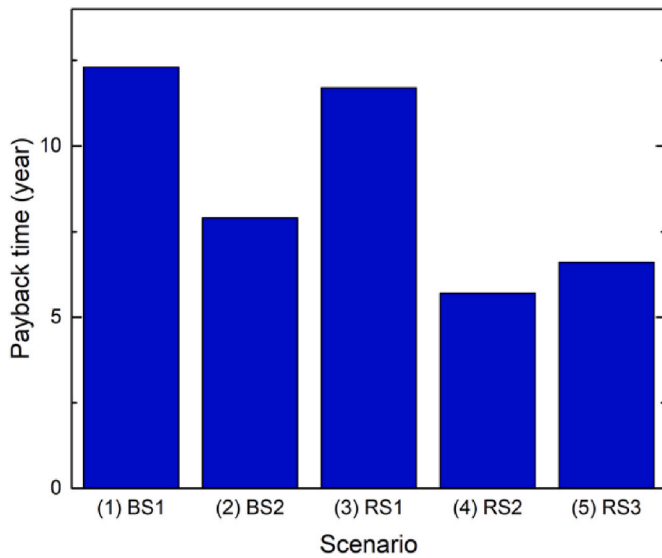


Fig. 5. Payback time of each fixture scenario (in years).

Table 12 Results from the EROI and EPBT of three potential situations.

		EROI	EPBT
Substitution	15 years	7.6	1.98 years
	25 years	12.5	
	30 years	15	
Reparation	15 years	7544	0.002 years
	25 years	12,780	
	30 years	15,513	
Do-nothing alternative		n.a.	n.a.
Reference for sc-Si and mc-Si modules [60]	30 years	14–16	0.6–1.5 years

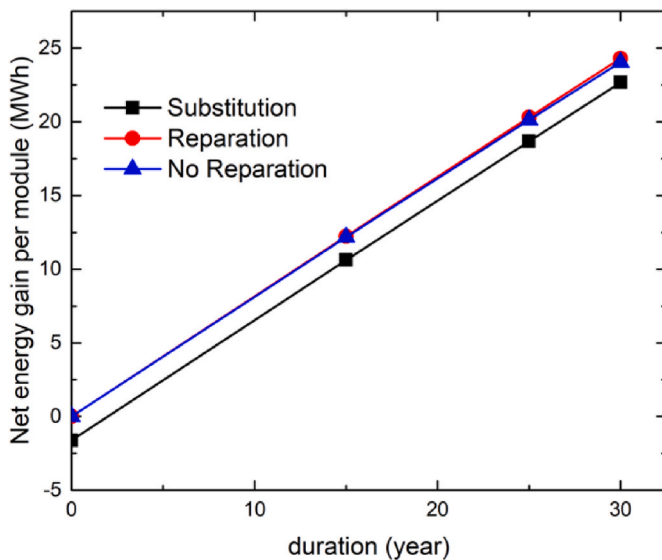


Fig. 6. The NEG to the energy system per module for the three potential situations (in MWh).

tested on performance and reliability. This repair scenario (RS1) or the substitution with a new PV module (BS1) comes at a cost. Their CPN/kWp distributions range between 6.12€ – 8.50€ (RS1) and 6.68€ – 8.53€ (BS1). These results are coherent with previous study by Eder et al. [37], who calculated a CPN/kWp of 8.3€ for glass breakage. The CPN calculation was made with substitution costs of 108€ per module, whereas the cost for the research specimen was 90–95€ [44]. The costs for

substitution or repair products significantly impact the outcome of the CPN. Substitution can make use of initial module costs when additional modules were directly ordered. However, the costs of reordering can be substantially higher, especially when small amounts or customized PV modules are required [44].

Surprisingly, the performance loss and multiplier variables barely impact the CPN outcome, even though the complete ranges were applied to prevent underestimation of costs due to reduced electricity generation. Beforehand, it was expected that the CPN results from scenarios BS1 and RS3 would be significantly lower due to exclusion of downtime. However, the appropriate explanation for the lower CPNs is the reduced worktime since uninstallation is not required. Reparation scenario RS3 is estimated to be less expensive (4.24 €/kWp/year) than substitution scenario BS2 (5.03 €/kWp/year).

4.5. NPV and PBT

The fixture scenarios for installed PV modules scenario (1) BS1 and (3) RS1 are the least attractive options in economic terms, due to the highest costs. Their NPV per module is 42€ for substitution (1) BS1 and 50€/per module for reparation (3) RS3, see Fig. 4. These results are both significantly less profitable than reparation scenario (4) RS2, 153€/per module, which is the most economically attractive scenario overall. Scenarios for uninstalled PV modules, (4) RS2 and (2) BS2, demonstrate noteworthy results with net present values of 136€/per module (4) RS2 and 113€/per module (2) BS2, respectively. The opposite distribution is perceived in Fig. 5, which visualizes PBT results of fixture scenarios. Scenarios (1) BS1 and (3) RS1 rely on their profitability in the final years of the subsidy (PBT of 12.3 and 11.7 years), whereas scenarios (2) BS2, (4) RS2 and (5) RS3 become profitable after 7.9 years, 5.7 years and 6.6 years. Reparation or substitution of PV modules at projects that have been operating for a long period may therefore be economically challenging.

4.6. Energy to the system

The double-glass PV specimen has an invested energy of 1633 kWh/per module (986 kWh/m<sup>2</sup>) [63], whereas the invested energy for the glass repair resin is calculated at 1.51 kWh/per module reparation [63]. Obviously, the do-nothing alternative does not require any energy investments. The sizeable difference in invested energy creates a gap in EPBT and EROI. The EPBT in the substitution situation is 1.98 years, whereas the reparation requires less than one day (0.002 years) to return the invested energy to the system. The insignificance of the invested energy in repair resin is likewise displayed in the EROI of the reparation situation, see Table 12. The results clearly show that reparation is on a different NEA scale than the substitution of PV modules, emphasizing the impact a simple reparation can make. Fig. 6 shows the NEG of the three situations. The most net energy to the system is provided by reparation, with 24.3 MWh per module in 30 years. The applied degradation rate of the do-nothing scenario is derived from the DH test results and slightly higher than the rate of substitution and reparation. However, the NEG curves for all three situations are running roughly parallel, see Fig. 6, the difference in degradation rate has minimal impact.

5. Conclusions

Solar photovoltaic (PV) energy is a crucial supply technology in the envisioned renewable energy system. With enormous amounts of PV modules being installed, some will be affected by early-life failures and the resulting e-waste from PV modules is raising environmental concerns. A failure of growing importance is the defect in the glass layer(s) of glass-glass PV modules. In this research we applied an experimental repair technique for glass defects at these glass-glass PV modules. The effectiveness of the repair technique was analyzed using several performance and reliability tests, that were conducted after accelerated lifetime (damp heat) simulation. Furthermore, the research analyzed the economic and energetic

impact of glass defect repair in comparison with regular substitution.

We found that glass-glass PV modules which endured glass defects did not show performance loss, nor internal damage to the PV cells. These results were expected, since glass-glass PV modules are resilient to cell breakage and glass defects are expected to cause degradation over time. Furthermore, the reparation technique did not impose additional problems on the PV modules and can therefore be considered harmless. Finally, the repaired PV modules performed properly during and after the DH test. The absence of water-instigated degradation indicates that repaired glass layers are insulating again. However, definite conclusions must be made with caution since the non-repaired PV modules did not show visual signs of water ingress either. The combination of impermeable glass layers (except for the cracks) and the low WVTR of the POE encapsulant might be an inhibitory factor for visual effects for the ingress of water. Overall, the first indicators for a technically feasible and effective repair technique are positive.

A more definite conclusion can be made on the energetic impact of glass reparation. The NEA results clearly show that reparation is on a different scale than the substitution of PV modules, emphasizing the impact a simple reparation can make. Therefore, this research concludes that reparation is energetically desirable. The economic indicators were not as distinctive and are sensitive to the practical application of the repair technique. The PV failure costs (CPN/kWp) are dominantly affected by the 'time to fix' and the 'costs of materials', other variables were negligible. The reparation costs are expected to decrease with an increase in scale and frequency of glass defects. Furthermore, the costs of reordering for substitution can be substantially higher, especially when small amounts or customized PV modules are required. Therefore, glass defect reparation may be economically interesting in the future.

Finally, the experimental glass defect reparation technique shows promising results, both on the technical feasibility and effectiveness as on the energetic and economic contribution. To gain more understanding about the technical feasibility, several reliability tests should be conducted such as the mechanical load and humidity-freeze tests. Followed by in-depth studies with sufficiently CPN/kWp large sample sizes and

comprehensive accelerated test series. Furthermore, the economic viability must prove its potential when the technique is standardized and applicable on both scale and frequency. Ultimately, the results of this research underline the opportunities that will arise in the EoL pathways of PV modules and hopefully place defects at PV modules in a different perspective.

#### CRediT authorship contribution statement

**Mathijs Tas:** Writing – original draft, Visualization, Software, Methodology, Investigation, Formal analysis, Data curation, Conceptualization. **Wilfried G.J.H.M. van Sark:** Writing – review & editing, Writing – review & editing, Visualization, Supervision, Conceptualization.

#### Declaration of competing interest

The authors declare that they have no known competing financial interests or personal relationships that could have appeared to influence the work reported in this paper.

#### Data availability

Data will be made available on request.

#### Acknowledgements

The authors would like to thank SolSolutions for taking initiative in this research and for supplying defective and reference PV modules, furthermore the authors acknowledge the contribution from TNO, in particular Martin Späth, Maurice Goris and Peter Blokker, who arranged the thorough testing of the repair technique. Finally, we would like to extend our gratitude to Marcel Falk from GlasGarage for his help and expertise on the reparation technique and DMEGC Solar for sharing valuable information on the specimen.

## Appendix A. IEC Standards

This appendix details the various IEC standards [41] that are of relevance in this work.

### A.1 IEC 61215

The IEC 61215 standard is the most widely used standard for PV modules and consists of a series of Module Quality Tests (MQTs) which together determine the design approval, qualification process and type approval of terrestrial PV modules. The IEC 61215 standard verifies the suitability of terrestrial PV modules for a long-term operation in open-air climates [67]. The MQTs are divided into five sequences. These sequences each check the PV modules on the main degradation modes based on performance-, electrical-, thermal-, diagnostic test, environmental- and mechanical parameters [67]. After the five distinct test sequences, PV modules are once more subject to the initial efficiency tests. The final criteria for PV modules are [67].

- a) Maximum power output degradation on each test is limited to  $\leq 8\%$
- b) No open circuits during tests
- c) No visual evidence for major defects
- d) Insulation test requirements are met
- e) Wet leakage test is fulfilled successful
- f) Specific test requirements are met

PV module designs that fulfill all sequences and meet the final criteria are IEC 61215 tested. However, this is a guideline and actual certification is based on (inter)national and performed by specialized companies.

### A.2 IEC 61730

The IEC 61730 standard specifies and describes the requirements to provide the safe electrical and mechanical operation of terrestrial PV modules, each module design is classified based on their safety qualification. The IEC 61730 standard is focused to minimize issues associated with wrongly installed PV modules that can cause fire hazards, electrical shock or potential injury. These criteria are tested under artificially created mechanical and environmental stress [68]. The modules are categorized into four classes that correlate with the IEC 61140 application classes. The IEC 61140



determines the protection against electrical shocks [69].

**Table A1**  
Overview and description of the correlating IEC 61140 and IEC 61730 classes

IEC 61140	IEC 61730	Description
Class 0	Class B	PV modules/systems in restricted access area
Class I	Not covered in IEC 61730 standard	Special installation requirements
Class II	Class A	PV modules/systems in non-restricted access area
Class III	Class C	Limited voltage (ELV) creates basic protection

The glass-glass PV specimen in this research can generate electrical (system and individual module) outputs at hazardous voltage, current and power levels and are therefore categorized in safety class A.

### 2.4.3. IEC 61440

The IEC 61140 standard defines the electrical protection class of electrical devices, which in term determines the requirements for electrical safety under e.g. short circuit or lightning circumstances. IEC 61140 is a general electrical safety standard and not specifically prepared for PV modules [69]. The tests series for IEC 61730 subsequently define the protection classes for PV modules in IEC 61440. The glass-glass PV specimen in this research are categorized in protection class II.

## Appendix B. CPN Calculations

$$CPN = C_{down} + C_{fix} \quad (B1)$$

$$CPN / kWp = \frac{C_{down} + C_{fix}}{N_{Comp} \times W_{module}} \quad (B2)$$

$$L = O_{CPN} \times S_{CPN} \quad (B3)$$

$$N_{fail,year} = N_{fail} \times 100 \quad (B4)$$

$$T_{down,fail} = T_{dec} \times T_{tr/ts} \times PL \times M + T_{fix} \times M \quad (B5)$$

$$T_{down} = T_{down,fail} \times N_{fail} \quad (B6)$$

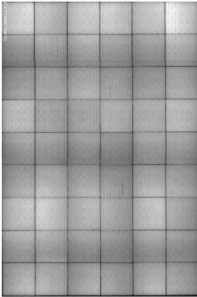
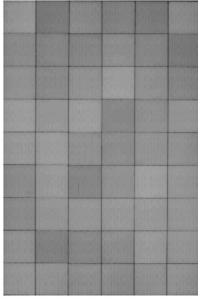
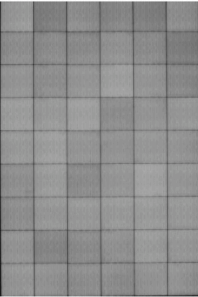
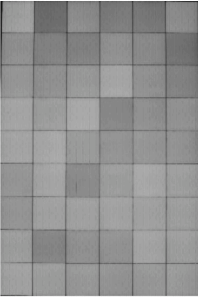
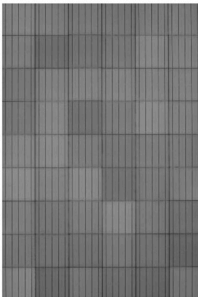

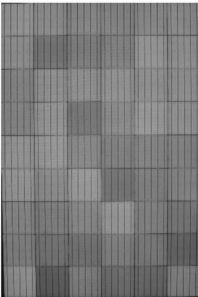
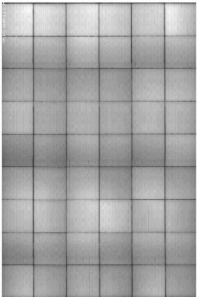
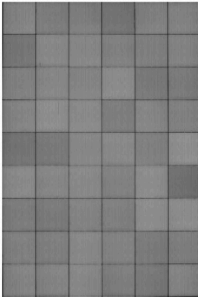
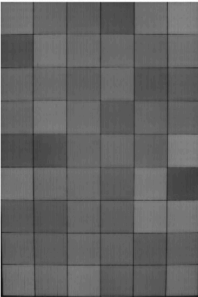
$$T_{down,comp} = T_{down} / N_{comp} \quad (B7)$$

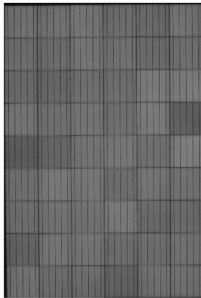
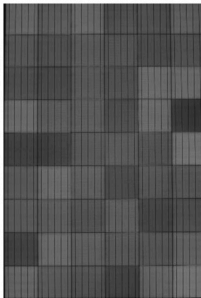
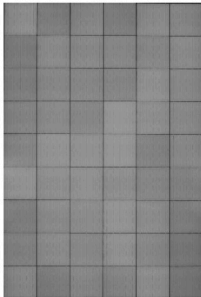
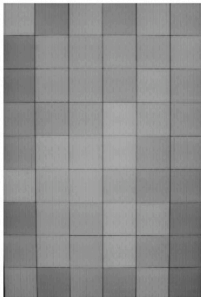
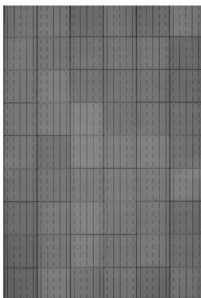
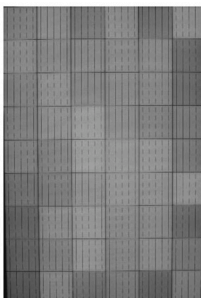
$$O_{CPN} = T_{down,comp} / T_{ref} \quad (B8)$$

$$S_{CPN} = N_{comp} \times W_{module} \quad (B9)$$

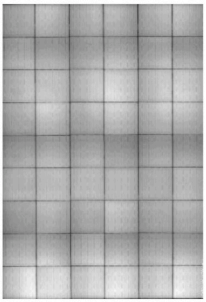
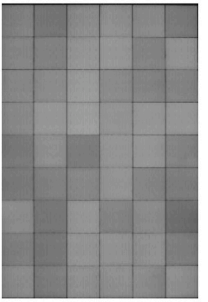
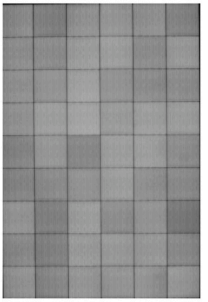
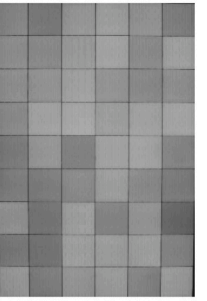
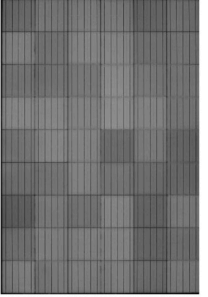
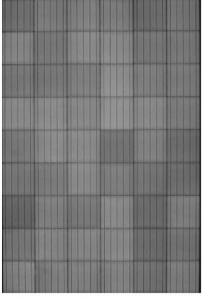
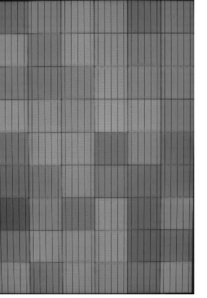
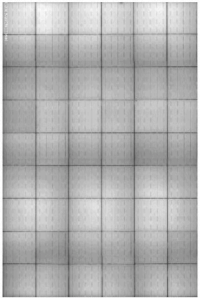
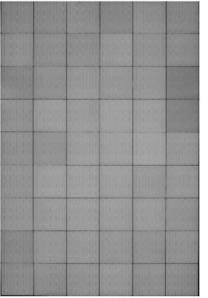
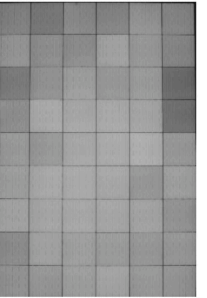
## Appendix C. EL images

EL images of the research specimen.

<b>Manufacturer</b> (DMEGC, China)	<b>Initial EL test</b> (TNO, Petten)	<b>After Reparation</b> (TNO, Petten)	<b>After damp-heat exposure</b> (TNO, Petten)
Specimen 1 – frontside 			
Specimen 1 – rearside Not applicable			
Specimen 2 – frontside 		Not applicable	

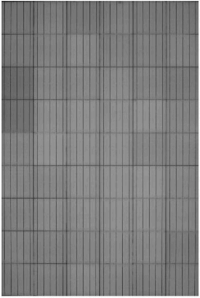
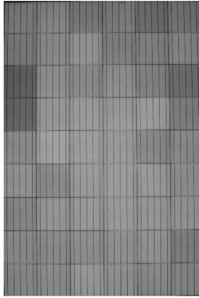
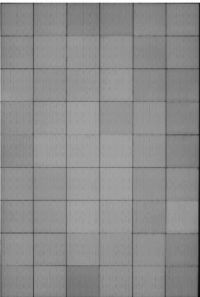
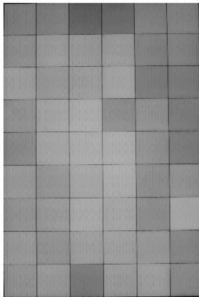
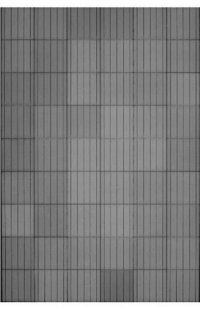
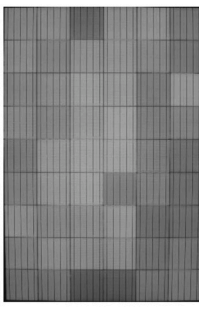
Specimen 2 – rearside Not applicable		Not applicable	
Specimen 3 – frontside		Not applicable	
Specimen 3 – rearside Not applicable		Not applicable	

. (continued).

Specimen 4 - frontside 			
Specimen 4 – rearside Not applicable			
Specimen 5 – frontside 		Not applicable	

. (continued).

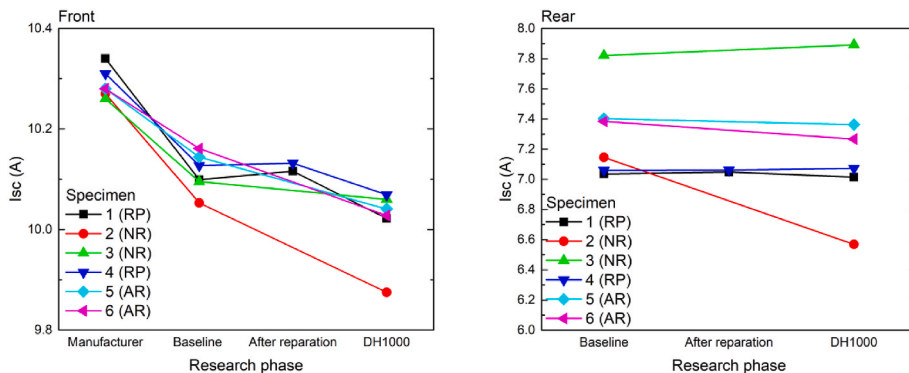


Specimen 5 – rearside Not applicable		Not applicable	
Specimen 6 – frontside		Not applicable	
Specimen 6 – rearside Not applicable		Not applicable	

. (continued).

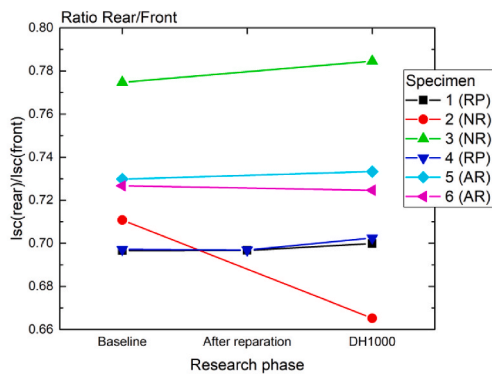
**Appendix D. Performance parameters**

Performance parameters Isc (A), Voc (V), Impp (A), Vmpp (V) and fill factor for front and rear illumination at various stages of the research.



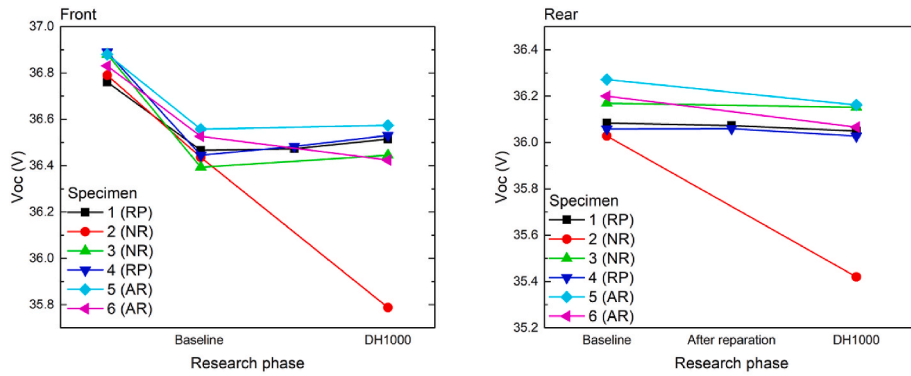
(a)

(b)



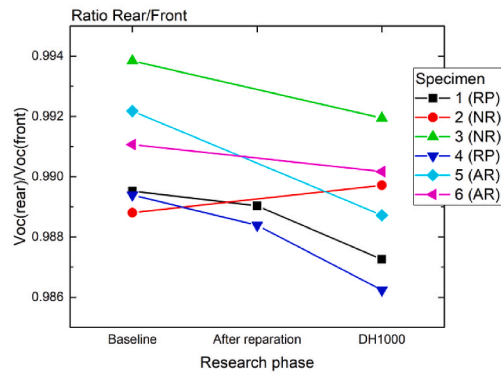
(c)

**Fig. D1.** Measured short circuit current Isc (A) of the various PV modulea at each phase of the research phase, (a) front side, (b) rearside, and (c) power ratio of rear to front side. The black and dark blue lines (specimens 1 and 4), represent the repaired PV modules. The read and green lines (specimen 2 and 3), the non-repaired PV modules, and the light blue and purple lines (specimen 5 and 6), are the as-received (reference) PV modules.



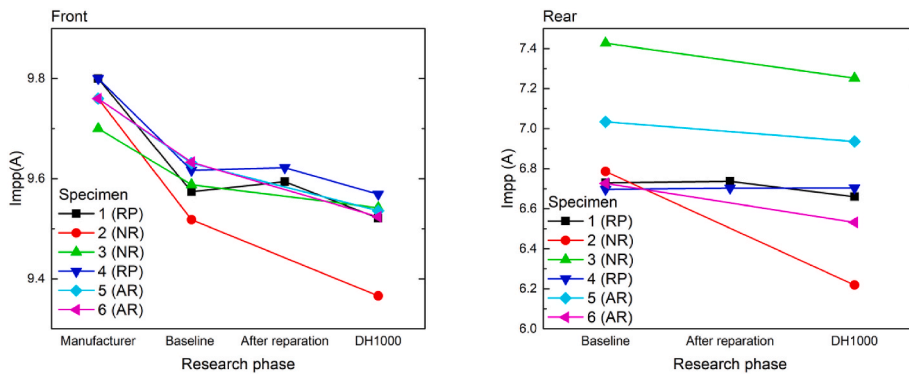
(a)

(b)



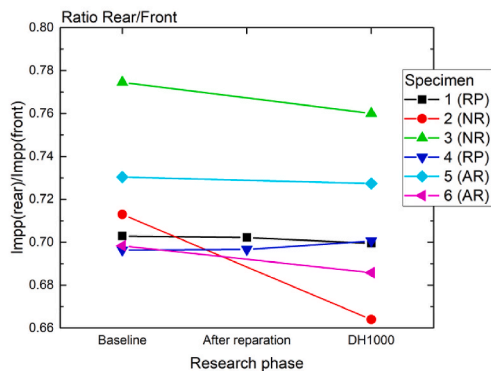
(c)

**Fig. D2.** Measured open circuit voltage  $V_{oc}$  (V) of the various PV modulea at each phase of the research phase, (a) front side, (b) rearside, and (c) power ratio of rear to front side. The black and dark blue lines (specimens 1 and 4), represent the repaired PV modules. The read and green lines (specimen 2 and 3), the non-repaired PV modules, and the light blue and purple lines (specimen 5 and 6), are the as-received (reference) PV modules.



(a)

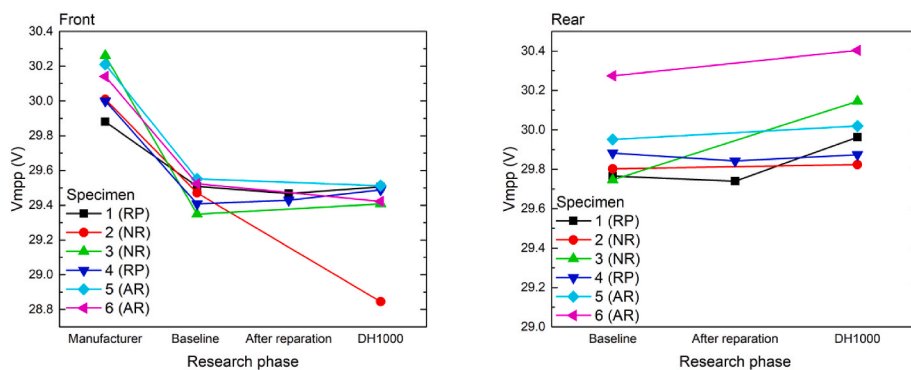
(b)



(c)

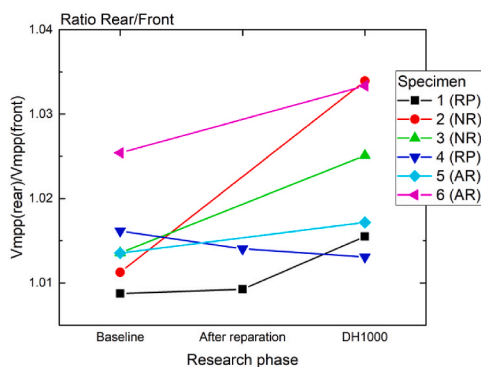
**Fig. D3.** Measured current at maximum power  $I_{mpp}$  (A) of the various PV modulea at each phase of the research phase, (a) front side, (b) rearside, and (c) power ratio of rear to front side. The black and dark blue lines (specimens 1 and 4), represent the repaired PV modules. The read and green lines (specimen 2 and 3), the non-repaired PV modules, and the light blue and purple lines (specimen 5 and 6), are the as-received (reference) PV modules.





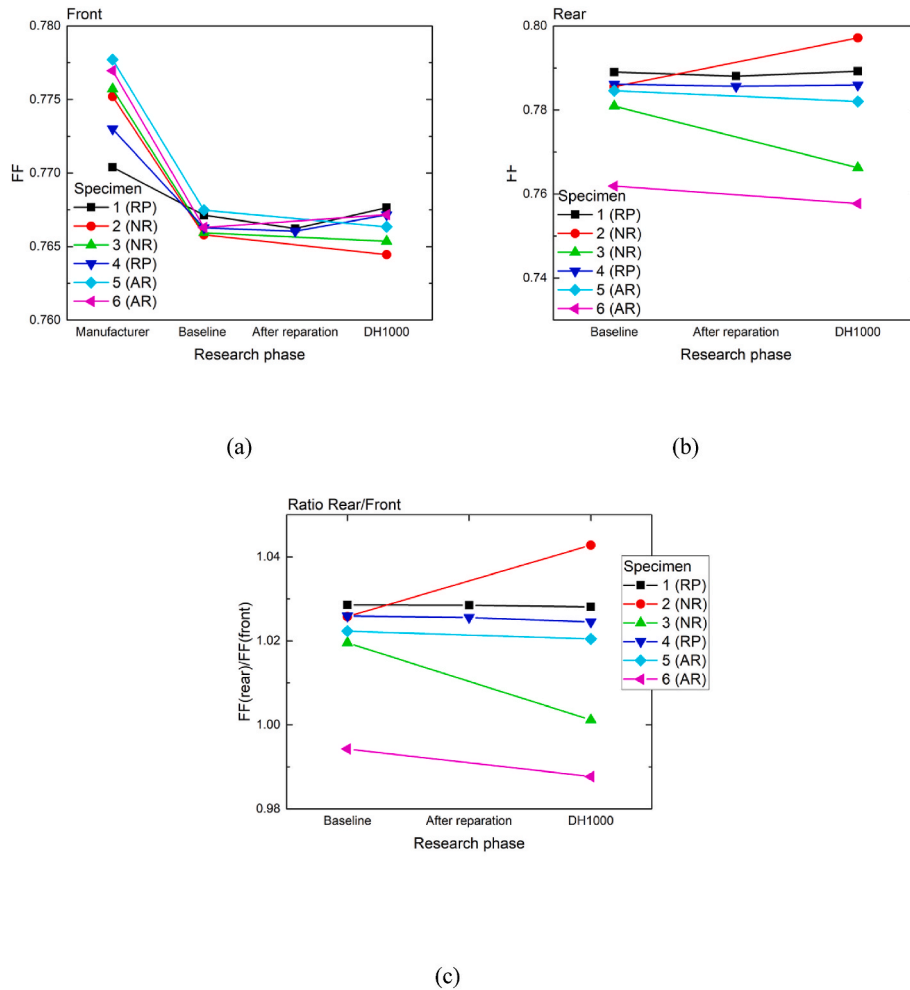
(a)

(b)



(c)

**Fig. D4.** Measured voltage at maximum power  $V_{mp}$  (V) of the various PV modulea at each phase of the research phase, (a) front side, (b) rearside, and (c) power ratio of rear to front side. The black and dark blue lines (specimens 1 and 4), represent the repaired PV modules. The read and green lines (specimen 2 and 3), the non-repaired PV modules, and the light blue and purple lines (specimen 5 and 6), are the as-received (reference) PV modules.



**Fig. D5.** Measured fill factor FF of the various PV modulea at each phase of the research phase, (a) front side, (b) rearside, and (c) power ratio of rear to front side. The black and dark blue lines (specimens 1 and 4), represent the repaired PV modules. The read and green lines (specimen 2 and 3), the non-repaired PV modules, and the light blue and purple lines (specimen 5 and 6), are the as-received (reference) PV modules.

## References

- [1] IEA, World energy outlook 2020, International Energy Agency (2020). <https://www.iea.org/reports/world-energy-outlook-2020>. (Accessed 23 February 2023).
- [2] IPCC, Global warming of 1.5 °C, special report, International Panel on Climate Change (2018). <https://www.ipcc.ch/sr15/>. (Accessed 23 February 2023).
- [3] IEA, Renewables 2019, market analysis and forecast from 2019 to 2024, international energy agency. <https://www.iea.org/reports/renewables-2019>, 2019. (Accessed 23 February 2023).
- [4] K.Y. Youn, S.K. Hyun, T. Tam, K.H. Sung, J.K. Myong, Recovering valuable metals from recycled photovoltaic modules, *J. Air Waste Manag. Assoc.* 64 (7) (2014) 797–807.
- [5] M. Redlinger, R. Eggert, M. Woodhouse, Evaluating the availability of gallium, indium, and tellurium from recycled photovoltaic modules, *Sol. Energy Mater. Sol. Cell.* 138 (2015) 58–71.
- [6] J.R. Duflou, J.R. Peeters, D. Altamirano, E. Bracquene, W. Dewulf, Demanufacturing photovoltaic panels: comparison of end-of-life treatment strategies for improved resource recovery, *CIRP Annals* 67 (1) (2018) 29–32.
- [7] IRENA, End-of-Life management – solar photovoltaic panels, international renewable energy agency (IRENA) and international energy agency – photovoltaic power systems (IEA-PVPS). <https://www.irena.org/publications/2016/Jun/End-of-life-management-Solar-Photovoltaic-Panels>, 2016. (Accessed 23 February 2023).
- [8] A. Divya, T. Adish, P. Kaustubh, P.S. Zade, Review on recycling of solar modules/panels, *Sol. Energy Mater. Sol. Cell.* 253 (2023) 112151.
- [9] T.L. Curtis, H. Buchanan, L. Smith, G. Heath, A circular economy for solar photovoltaic system materials: drivers, barriers, enablers, and U.S. Policy considerations, National Renewable Energy Laboratory (2021). <https://www.osti.gov/biblio/1774574>. (Accessed 23 February 2023).
- [10] ITRPV, International technology roadmap for photovoltaic (ITRPV), 2021 results. <https://www.vdma.org/international-technology-roadmap-photovoltaic>, 2022. (Accessed 23 February 2023).
- [11] P. Verlinden, Advanced module concepts, chapter 10.4, in: A. Reinders, P. Verlinden, W. Van Sark, A. Freundlich (Eds.), *Photovoltaic Solar Energy: from Fundamentals to Applications*, Wiley, 2017.
- [12] IEA-PVPS, Review of failures of photovoltaic modules. International energy agency photovoltaic power systems (IEA-PVPS), Report T13-01 2014 (2014). <https://iea-pvps.org/key-topics/review-of-failures-of-photovoltaic-modules-final/>. (Accessed 23 February 2023).
- [13] M. Aghaei, A. Fairbrother, A. Gok, S. Ahmad, S. Kazim, K. Lobato, G. Oreski, A. Reinders, J. Schmitz, M. Theelen, P. Yilmaz, J. Kettle, Review of degradation and failure phenomena in photovoltaic modules, *Renew. Sustain. Energy Rev.* 159 (2022) 112160.
- [14] A. Ndiaye, A. Charki, A. Kobi, C.M.F. Kébé, P.A. Ndiaye, V. Sambou, Degradations of silicon photovoltaic modules: a literature review, *Sol. Energy* 96 (2013) 140–151.
- [15] S. Chen, M. Zang, D. Wang, S. Yoshimura, T. Yamada, Numerical analysis of impact failure of automotive laminated glass: a review. *Composites Part B: Engineering* 122 (2017) 47–60.
- [16] M. Overend, C. Louter, The effectiveness of resin-based repairs on the inert strength recovery of glass, *Construct. Build. Mater.* 85 (2015) 165–174.
- [17] S. Mahmoudi, N. Huda, M. Behnia, Critical assessment of renewable energy waste generation in OECD countries: decommissioned PV panels. *Resources, Conserv. Recycl.* 164 (2021) 105145.
- [18] G. Cattaneo, A. Faes, H. Li, F. Galliano, M. Gragert, Y. Yao, M. Despeisse, C. Ballif, Lamination process and encapsulation materials for glass-glass PV module design, *Photovoltaics International* (2015) 1–8.
- [19] J.P. Singh, S. Guo, I.M. Peters, A.G. Aberle, T.M. Walsh, Comparison of glass/glass and glass/backsheet PV modules using bifacial silicon solar cells, *IEEE J. Photovoltaics* 5 (3) (2015) 783–791.

- [20] M. Martin, X. Centelles, A. Solé, C. Barrenche, A.I. Fernandez, L.F. Cabeza, Polymeric interlayer materials for laminated glass: a review, *Construct. Build. Mater.* 230 (2020) 116897.
- [21] P. Sinha, A. Wade, Assessment of leaching tests for evaluating potential environmental impacts of PV module field breakage, *IEEE J. Photovoltaics* 5/6 (2015) 1710–1714.
- [22] J.H. Wohlgemuth, S. Kurtz, Reliability testing beyond qualification as a key component in photovoltaic's progress toward grid parity, *IEEE 2011 Intern. Reliability Physics Sympo. Monterey* 5E (3) (2011) 1–6.
- [23] S.N. Venkatesh, V. Sugumaran, Fault diagnosis of visual faults in photovoltaic modules: a Review, *Int. J. Green Energy* 18 (1) (2021) 37–50.
- [24] J.A. Tsanakas, A. van der Heide, T. Radavičius, J. Denafas, E. Lemaire, K. Wang, J. Poortmans, E. Voroshazi, Towards a circular supply chain for PV modules: review of today's challenges in PV recycling, refurbishment and re-certification, *Prog. Photovoltaics Res. Appl.* 28 (6) (2019) 454–464.
- [25] D.C. Jordan, T.J. Silverman, J.H. Wohlgemuth, S.R. Kurtz, van Sant, K. T, Photovoltaic failure and degradation modes, *Prog. Photovoltaics Res. Appl.* 25 (2018) 318–326.
- [26] H. Changwoon, N. Park, J. Jeong, Lifetime prediction of silicon PV module ribbon wire in three local weathers, Presentation at NREL 2012 Photovoltaic Module Reliability Workshop (2012).
- [27] Iea-Pvps, Assessment of photovoltaic module failures in the field. International energy agency photovoltaic power systems (IEA-PVPS), Report T13-09 2017 (2017). <https://iea-pvps.org/key-topics/report-assessment-of-photovoltaic-module-failures-in-the-field-2017/>. (Accessed 23 February 2023).
- [28] IEA-PVPS, Richter, Schadensbilder nach Wareneingang und im Reklamationsfall, 8, Workshop "Photovoltaik-Modultechnik", TÜV Rheinland (2014).
- [29] D. De Graaff, R. Lacerda, Z. Campeau, Degradation Mechanisms in Si Module Technologies Observed in the Field; Their Analysis and Statistics, Presentation at NREL 2011 PV Module Reliability Workshop, Golden, Colorado, 2011.
- [30] J.H. Wohlgemuth, M.D. Kempe, Equating damp heat testing with field failures of PV modules, in: Conference Record of the IEEE Photovoltaic Specialists Conference, 2013, pp. 126–131.
- [31] Y. Zhang, T. Dun, J. Du, X. Liu, H. Li, Q. Dong, T. Liu, Y. Huang, H. Jia, Y. Mai, How double glass laminated amorphous silicon solar modules break in the field: a case study, in: Conference Record of the 39th IEEE Photovoltaic Specialists Conference, 2013, pp. 3279–3283.
- [32] T.C. Felder, K.R. Choudhury, L. Garreau-Iiles, S. MacMaster, H. Hu, W.J. Gambogi, T.J. Trout, Analysis of glass-glass modules, *Proc. SPIE: New concepts in Solar and Thermal Radiation Conversion and Reliability* (2018), 107590E.
- [33] B. Weller, L. Tautenhahn, Mechanical challenge of frameless PV-modules, *Proce. Chall. Glass 2 – Conference on Archite.Structural Appli.Glass* (2010) 525–532.
- [34] M. Späth, Personal Communication with Martin Späth – Senior Researcher at TNO, 2020.
- [35] V. Gupta, M. Sharma, R. Pachauri, K.N.D. Babu, Impact of hailstorm on the performance of PV module: a review, *Energy Sources, Part A: Recovery, Utilization, Environ. Eff.* 43 (20) (2019) 2529–2543.
- [36] M.H. Hwang, Y.G. Kim, H.S. Lee, Y.D. Kim, H.R. Cha, A study on the improvement of efficiency by detection solar module faults in deteriorated photovoltaic power plants, *Appl. Sci.* 11 (2) (2021) 1–16.
- [37] G.C. Eder, Y. Voronko, C. Hirschl, R. Ebner, G. Újvári, W. Mühleisen, Non-destructive failure detection and visualization of artificially and naturally aged PV modules, *Energies* 11 (5) (2018) 1–14.
- [38] M. Abdelhamid, R. Singh, M. Omar, Review of microcrack detection techniques for silicon solar cells, *IEEE J. Photovoltaics* 4 (1) (2014) 514–524.
- [39] M. Bdour, Z. Dalala, M. Al-Addous, A. Radaideh, A. Al-Sadi, A comprehensive evaluation on types of microcracks and possible effects on power degradation in photovoltaic solar panels, *Sustainability* 12 (16) (2020) 6416.
- [40] S. Deng, Z. Zhang, C. Ju, J. Dong, Z. Xia, X. Yan, T. Xu, G. Xing, Research on hot spot risk for high-efficiency solar module, *Energy Proc.* 130 (2017) 77–86.
- [41] P. Verlinden, W.G.J.H.M. Van Sark, List of international standards, chapter 13.4, in: A. Reinders, P. Verlinden, W. Van Sark, A. Freundlich (Eds.), *Photovoltaic Solar Energy: from Fundamentals to Applications*, Wiley, 2017.
- [42] D. Moser, M. Del Buono, U. Jahn, M. Herz, M. Richter, K. De Brabandere, Identification of technical risks in the photovoltaic value chain and quantification of the economic impact, *Prog. Photovoltaics Res. Appl.* 25 (7) (2017) 592–604.
- [43] D.M.E.G.C. Solar, Datasheet on DMG290B6A-54XT PV solar cells. DMEGC Solar. <https://solarmagazine.nl/u/webshop/dmegc-vdh-kaspaneel.pdf>, 2020. (Accessed 23 February 2023).
- [44] SolSolutions, Personal Communication with Leon Bruinen, SolSolutions, 2021.
- [45] J. Zhang, J. Lasne, Personal Communication with Jasmine Zhang and John Lasne – Manufacturers and Researchers at DMEGC, 2021.
- [46] NOVUS, Document from NOVUS on windshield repair, Shared by personal communication with Gento van der Sanden, expert in windshield repairation (1991), 15-12-2020.
- [47] M. Falk, Personal Communication with Marcel Falk – Glass Repairation Expert at GlasGarage, 2021.
- [48] Iea-Pvps, Review on infrared and electroluminescence imaging for PV field applications. International energy agency photovoltaic power systems (IEA-PVPS), Report T13-10 2018 (2018). <https://iea-pvps.org/key-topics/review-on-ir-and-el-i-maging-for-pv-field-applications/>. (Accessed 23 February 2023).
- [49] G. Benatto, C. Mantel, S. Spataru, Santamaria Lancia, A. A. N. Riedel, S. Thorsteinson, P.B. Poulsen, H. Parikh, S. Forchhammer, D. Sera, Drone-based daylight electroluminescence imaging of PV modules, *IEEE J. Photovoltaics* 10 (3) (2020) 872–877.
- [50] Z. Xiong, T.M. Walsh, A.G. Aberle, PV module durability testing under high voltage biased damp heat conditions, *Energy Proc.* 8 (2011) 384–389.
- [51] Sde+, SDE+ voorjaar 2020, Ministerie van Economische Zaken en Klimaat (EZK) (2020). <https://www.rvo.nl/sites/default/files/2020/03/Brochure-SDE%20Voorjaar%202020-RVO%20NL.pdf> (Accessed 23 February 2023).
- [52] SecondSol (n.d.) Fixed costs for module repairation, <https://www.secondsol.com/nl/services/reparaturmodule.html> (last accessed 23 February 2023).
- [53] Van Gestel, Personal Communication with Rob Van Gestel, Founder of SolarTester and Specialized in Mobile Quality and Reliability Tests of PV Modules, 2021.
- [54] S. Lensink, M. Marsidi, L. Pisca, Eindadvies SDE++ 2021. Planbureau Voor Leefomgeving (PBL), 2021.
- [55] D. Moser, Personal Communication with Dr. David Moser – Research Group Leader at EURAC, Expert on Technical Risks at PV Projects, 2021.
- [56] A. Saltelli, Making best use of model evaluations to compute sensitivity indices, *Comput. Phys. Commun.* 145 (2) (2002) 280–297.
- [57] I.M. Sobol, Global sensitivity indices for nonlinear mathematical models and their Monte Carlo estimates, *Math. Comput. Simulat.* 55 (2001) 271–280.
- [58] J. Herman, W. Usher, SALib: an open-source Python library for sensitivity analysis, *J. Open Source Softw.* 2 (9) (2017) 97. <http://salib.github.io/SALib/>.
- [59] M. Ebrahimi, A. Keshavarz, CCHP evaluation criteria. Combined cooling, Heating and Power (2015) 93–102.
- [60] V. Fthenakis, E. Leccisi, Updated sustainability status of crystalline silicon-based photovoltaic systems: life-cycle energy and environmental impact reduction trends, *Prog. Photovoltaics Res. Appl.* 29 (2021) 1068–1077.
- [61] E. Leccisi, M. Raugi, V. Fthenakis, The energy and environmental performance of ground-mounted photovoltaic systems - a timely update, *Energies* 9 (8) (2016).
- [62] Iea-Pvps, Methodological Guidelines on Net Energy Analysis of Photovoltaic Electricity, International Energy Agency Photovoltaic Power Systems (IEA-PVPS), 2016. Report T12-07:2016, <https://iea-pvps.org/key-topics/task12-methodological-guidelines-on-net-energy-analysis-of-photovoltaic-electricity-2016/>. (Accessed 23 February 2023).
- [63] G. Wernet, C. Bauer, B. Steubing, J. Reinhard, E. Moreno-Ruiz, B. Weidema, The ecoinvent database version 3 (part I): overview and methodology; *Ecoinvent* (2021), *Int. J. Life Cycle Assess.* 21 (9) (2016) 1218–1230.
- [64] J. Yang, D. Lee, D. Baek, D. Kim, J. Nam, P. Huh, Effect of various encapsulants for frameless glass to glass Cu(In,Ga)(Se,S)<sub>2</sub> photovoltaic module, *RSC Adv.* 5 (63) (2015) 51258–51262.
- [65] J. Lindroos, H. Savin, Review of light-induced degradation in crystalline silicon solar cells, *Sol. Energy Mater. Sol. Cell.* 147 (2016) 115–126.
- [66] M. Goris, Personal Communication with Maurice Goris – PV Module Expert and Responsible for the PV Test Conditions at TNO Petten, 2021.
- [67] Iec 61215, Terrestrial Photovoltaic (PV) Modules - Design Qualification and Type Approval, 2021.
- [68] Iec 61730, Photovoltaic Compliance Testing, 2018.
- [69] Iec 61140, Protection against Electric Shock - Common Aspects for Installation and Equipment, 2016.